PHYSICAL REVIEW APPLIED 1, 051001 (2014)

Phononic-Crystal-Based Acoustic Sieve for Tunable Manipulations of Particles by a Highly Localized Radiation Force

Fei Li,[1] Feiyan Cai,[1] Zhengyou Liu,[2] Long Meng,[1] Ming Qian,[1] Chen Wang,[1] Qian Cheng,[3] Menglu Qian,[3] Xin Liu,[1] Junru Wu,[4] Jiangyu Li,[5] and Hairong Zheng[1,*]

[1]*Paul C. Lauterbur Research Center for Biomedical Imaging, Shenzhen Institutes of Advanced Technology, Chinese Academy of Sciences, Shenzhen 518055, China*

[2]*Key Laboratory of Artificial Micro/Nano-structures of Ministry of Education and School of Physics and Technology, Wuhan University, Wuhan 430072, China*

[3]*Institute of Acoustics, Tongji University, Shanghai 200092, China*

[4]*Department of Physics, University of Vermont, Burlington, Vermont 05405, USA*

[5]*Department of Mechanical Engineering, University of Washington, Seattle, Washington 98195, USA*

(Received 2 May 2014; published 11 June 2014)

The ability to manipulate microscale and nanoscale particles is highly desirable for various applications ranging from targeting drug delivery to additive manufacturing. Here we report an acoustic sieve that is capable of aligning, trapping, sorting, and transferring a large number of particles according to their size or mass density, all in a tunable manner. The concept is based on the highly localized periodic radiation force induced by the resonance transmission of an acoustic wave across a phononic crystal plate, a phenomenon analogous to the surface-phonon-enhanced optical force, yet the physical concept has not been explored in acoustics. The acoustic sieve demonstrates the effective manipulation of massive particles using an artificially engineered acoustic field by a phononic crystal, and it has potential application for a wide range of applications.

DOI: 10.1103/PhysRevApplied.1.051001

The ability to sort, sieve, and manipulate microscale and nanoscale particles, especially in a tunable manner, is highly desirable for various applications ranging from targeting drug delivery [1] to additive manufacturing [2]. A conventional sieve uses a mesh of fixed size for separating smaller particles from the particle mixture of various sizes, but it cannot sort out different materials of the same size and is incapable of particle manipulation. Optical [3–7] and acoustic [8–13] tweezers have been developed to trap and manipulate nanoparticles [14–16], biomolecules [17,18], and organisms [19], yet they can capture only a few particles at a time and are difficult to scale up. Here we introduce an acoustic sieve that can align, trap, sort, and transfer a large number of particles in a liquid according to their size or mass density, all in a tunable manner. This device not only overcomes the shortfalls of a traditional sieve and optical or acoustic tweezers, but also fulfills many more functionalities. Therefore, we call it an acoustic sieve.

The concept is motivated by the highly localized radiation force induced by the artificially engineered acoustic field in a phononic crystal plate (PCP), as suggested by our theoretical and numerical analysis [20,21]. It is thus distinct from other acoustic techniques that rely on standing waves or Gaussian beams directly generated by the acoustic transducer to trap one or several identical particles [8–13]. By controlling such a radiation force, a large number of particles can be manipulated, and the principle can be understood as follows. The zero-order antisymmetric A_0 mode of the Lamb wave is a flexural mode, which exists intrinsically in a uniform brass plate, and usually can be excited by an external ultrasound (US) wave in water at a high frequency. However, at a frequency f below the so-called "cutoff frequency," the corresponding phase velocity of the A_0 mode at f is smaller than that of US in water, and the consequent mismatch of momentum makes the coupling between the A_0 mode and US to diminish [20]. This A_0 mode thus becomes a nonleaky mode and strongly dispersive (the phase velocity is a function of frequency). However, the periodic stub structure (grating) of a PCP constructed on the top surface of a flat plate with a spatial period p [see Fig. 1(a)] equal to the wavelength of the A_0 mode makes the effective excitation of the A_0 mode of the plate possible. Physically, the Bragg scattering by the grating of the PCP folds the dispersion relation of the A_0 mode to the leaky range and therefore the match of momentum in the direction of the US propagation takes place [20]. It gives rise to a remarkable ultrasound transmission peak through the plate at the resonance frequency of the A_0 mode [20]; the measured spatially averaged acoustic power of the incident US beam transmitted through the plate reaches 60% [see Fig. 1(b)] at the resonance frequency (1.282 MHz) using a 2-cm-diameter nonfocusing US transducer. Such a resonance transmission and highly localized field below the plate surface induce a large acoustic radiation force that can be utilized to trap and

*Corresponding author.
hr.zheng@siat.ac.cn

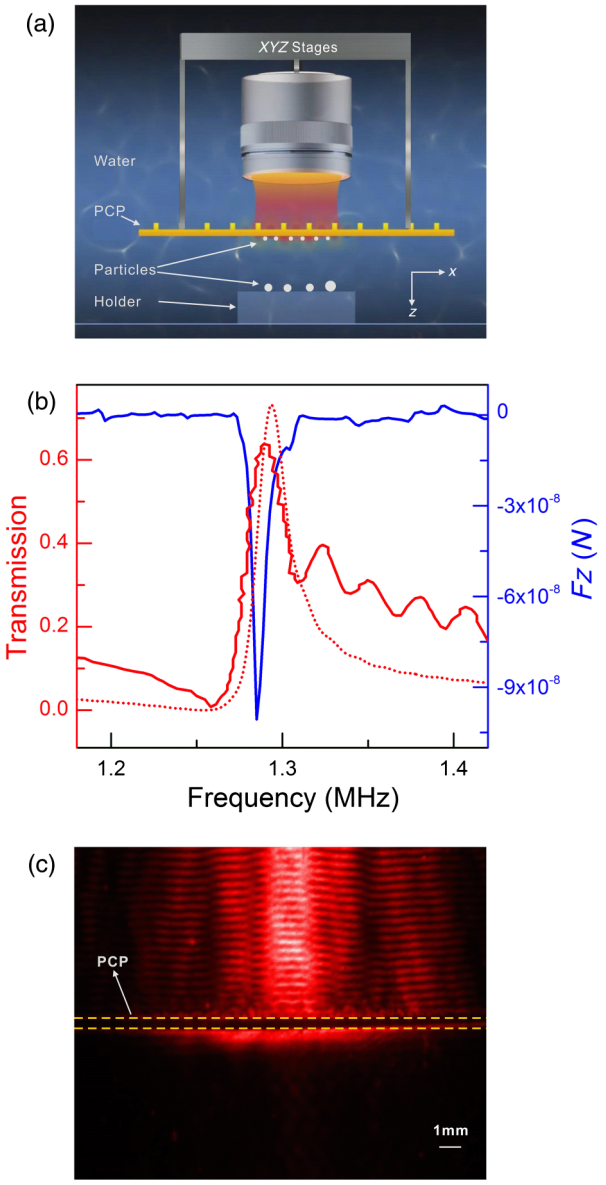

FIG. 1. Illustration of an acoustic sieve. (a) The experimental setup comprises a weakly focusing ultrasound (US) transducer with a center frequency of 1.22 MHz, a PCP with periodically distributed stubs (gratings) of rectangular shape (spatial period $p = 820\ \mu$m, width $w = 120\ \mu$m, height $h = 120\ \mu$m) constructed on the top surface of a flat uniform brass plate (thickness $t = 180\ \mu$m) by the laser etching technique. Particles randomly distributed on a plastic specimen holder which is transparent for both acoustic and electromagnetic (light) waves. (b) The experimentally measured (solid line in red), numerical calculated (dotted line in red) normalized acoustic power transmissions and the numerical calculated acoustic radiation force exerted on a glass sphere of diameter 200 μm with a vertical distance of 30 μm to the flat surface of PCP (in blue) are shown as a function of frequency when the acoustic beam is normally incident upon the PCP from the top; the measured transmission peak frequency agrees well with computational natural frequency (1.282 MHz) of the A_0 mode of the plate. (c) An image of the instant acoustic pressure field near the PCP at the resonance frequency is obtained by the Schlieren technique.

manipulate particles, a phenomenon analogous to the surface plasmon enhanced optical force [22], yet the physical concept has not been explored in acoustics. It is noted that if the PCP with the grating structure is not mounted on the flat brass plate of the same thickness, the acoustic power transmitted through the plate is frequency independent and less than 10% between 1.1 and 1.5 MHz due to mismatch of acoustic impedances between water and brass [23].

We realize aligning, trapping, sieving, transferring, and releasing of subwavelength-scale (relative to the wavelength of US in water) particles by using a PCP and experimental setup (see Supplemental Material [24]) shown in Fig. 1(a). Figure 1(b) clearly reveals that the magnitude of a negative z-directional acoustic radiation force reaches the maximum and changes drastically, causing sharp gradients near the resonance frequency. The sharp-gradient pattern repeats periodically in the horizontal (x) direction near the plates. Furthermore, the image obtained by the Schlieren technique [25,26] in Fig. 1(c) shows that in the side view (x-z plane) of the instant spatial distribution of the acoustic pressure, the transmitted acoustic pressure is highly localized in the vertical (z) direction and diminishes rapidly within a short distance (approximately <1 mm) beyond the plate. All those features indicate that the transmission that occurred here is caused by the resonance transmission, fundamentally different from that of the ordinary mechanisms used by other researchers prior to this research.

A large number of particles can be simultaneously trapped by the acoustic sieve, as shown in Fig. 2. When the PCP bottom surface is placed in close proximity to the specimen holder, on which glass spheres with diameters of 150–210 μm are randomly located [see Fig. 2(a)], these spheres are trapped and aligned into a set of parallel lines in the y direction on the plate (x-y plane) with approximately $0.42p$ and $0.58p$ separations, alternately. The trapping is quite robust; when the plate with the PCP is moved away from the proximity of the specimen holder, the particles are still trapped on the plate [see Fig. 2(b)], as the trapping force combining with the buoyancy counteracts the effect of the gravity. The trapped particles can be stably transported together with the transducer-PCP system by the XYZ stages and can be released at a desired location by either reducing the incident acoustic power or tuning the driving frequency away from the resonance frequency. This process can also be observed clearly in Movie S1 in the Supplemental Material [24].

A detailed numerical analysis of the acoustic radiation force field near the PCP is carried out by using the three-dimensional finite-difference time-domain (FDTD) method combined with the momentum-flux tensor [27]. The positions of black arrows in Fig. 2(c) denote the stable trapping places of the particle under the plane surface of the PCP, where the magnitude of the x-directional acoustic

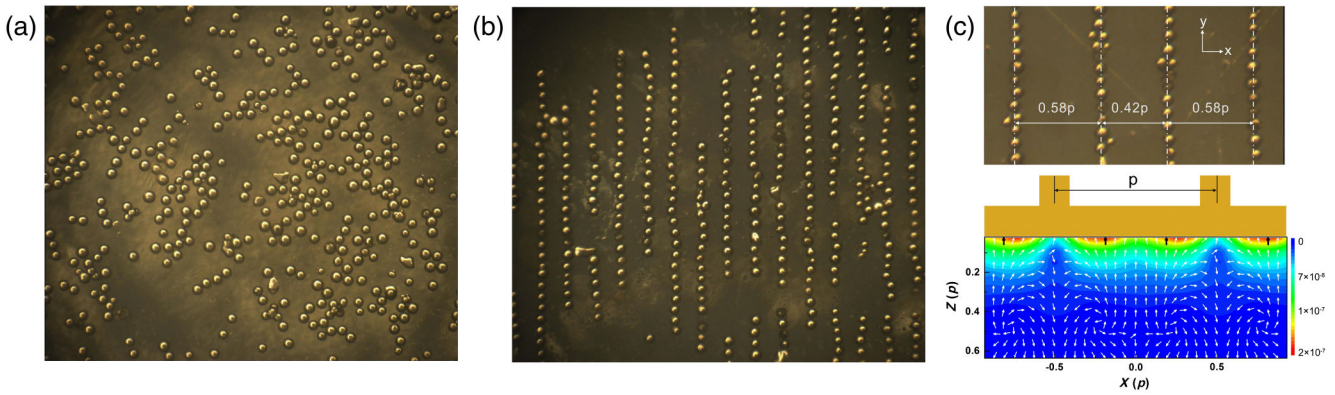

FIG. 2. Aligning, trapping, and releasing particles by PCP. (a) Glass spheres of 150–210 μm diameters are strewn on specimen holder. (b) The trapping of the glass spheres on the PCP surface is achieved by an incident acoustic wave propagating in the z direction with the acoustic power of 15.6 W and frequency of 1.282 MHz, matching the resonance frequency of the A_0 mode. (c) A segment of the brass plane shows glass spheres with diameter 70–100 μm trapped on the surface (the upper figure). The numerical map of x- and z-directional radiation forces exerted on a glass sphere with diameter 100 μm near the flat bottom side of the PCP at 1.28 MHz (the lower figure; color and arrow represent the magnitude and the direction, respectively). The positions of black arrows in the bottom figure represent the stable horizontal places of the particle at the bottom plane surface of the PCP. It is noted that the spacing between the first and second black arrows is about $0.6p$ and that between the second and third is about $0.4p$, which agrees well with the alternate intervals of trapping locations in the top figure.

radiation force diminishes and the magnitude of acoustic radiation trapping force along the negative-z direction reaches the maximum. It is observed that for this PCP there are two sets of distinct stable trapping positions; the spacing between two nearest neighbors is approximately $0.4p$ or $0.6p$, alternately, which agrees well with the experimental results as shown in Fig. 2(c).

Computational analysis shows that the trapping force is a function of the particle size, mass density, and the acoustic power of the incident wave [28], and this function enables sorting and sieving particles in a tunable manner by using different levels of acoustic power of the incident acoustic wave. The forces applied to a particle include gravity, buoyancy, x-directional, and z-directional acoustic radiation forces. It is noted that the buoyancy and gravity of a particle are cubic-power functions of its diameter and linear functions of its mass density, while the radiation force is a function of both density and size of particles as well, which was computed numerically by the FDTD method (see Supplemental Material [24]). The magnitude of the gravity minus buoyancy for the glass spheres versus diameter is shown in Fig. 3(a) (black line). When the radiation force curves corresponding to various acoustic powers are above the black solid line, particle trapping would take place. It is evident that, for this PCP structure, the particle with diameter smaller than 150 μm could be trapped when the acoustic power is over 5 W. When the acoustic power is larger than 10 or 20 W, the largest glass spheres to be trapped also increase to 350 or 550 μm, respectively. As such, we can selectively trap particles of desired sizes in a tunable manner. For example, if we want to trap particles between 150 and 350 μm, the appropriate acoustic power should be larger than 5 W but smaller than 10 W. The narrower the acoustic power range is, the narrower the size range is, and the targeted size range is tunable. This concept is confirmed by experimental results shown in Figs. 3(b)–3(d), which illustrate particle sieving of different diameters by the PCP using different acoustic power.

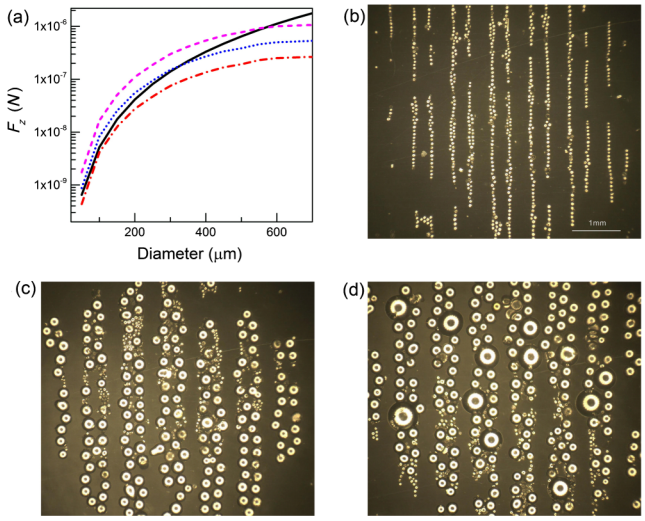

FIG. 3. Sieving particles according to their sizes. (a) The numerical magnitude of the z-directional acoustic radiation force as a function of the diameter and input acoustic power (red short dash dots, blue short dots, magenta short dashes represent input acoustic powers of 5, 10, and 20 W, respectively). The magnitude of gravity minus buoyancy for the glass spheres versus different particle diameters is shown by the solid black line. (b) Initially, only the glass spheres with diameters of 70–100 μm are trapped and aligned into parallel lines on the PCP at acoustic power of 4 W. (c) With acoustic power increased to 10.2 W, the glass spheres with diameters of 150–210 μm are also captured. (d) Finally, the glass spheres with diameters of 425–600 μm are trapped as well at 30.6 W.

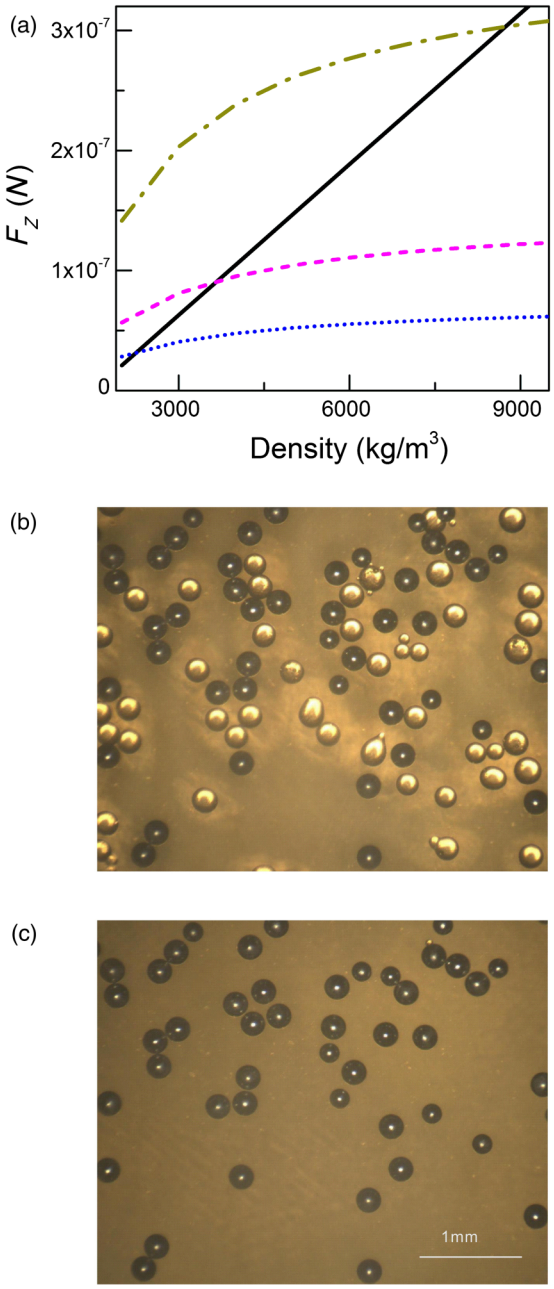

FIG. 4. Sieving particles according to their materials. (a) The computed magnitude of the acoustic radiation force as a function of the density of particle and input acoustic power (blue short dots, magenta short dashes, and dark yellow dash dots represent input acoustic powers of 10, 20, and 50 W, respectively). The magnitude of gravity subtracting buoyancy versus particle diameters is shown by the solid black line. (b) The trapping for the mixture of glass spheres with diameters of 230–300 μm and tin spheres with diameters of 210–250 μm at a frequency of 1.282 MHz and acoustic power of 39 W. The mixing particles are on the specimen holder before sieving. (c) All of the glass spheres are captured, and only tin spheres stay on the specimen holder after sieving.

In addition to sorting particles of different size, the acoustic sieve is also capable of sieving particles of different mass density but the same size. Figure 4(a) shows the numerically calculated magnitude of the acoustic radiation force as a function of the mass density of particles and input acoustic power, when the diameter of particle is 200 μm and longitudinal and transverse wave velocities of particle are the same as glass. The magnitude of gravity subtracting buoyancy for the glass spheres versus particle diameters is shown by the solid black line. It suggests that trapping would take place only if the radiation force curves of various acoustic powers are above the black solid line, making it possible to sieve particles of different density using different acoustic powers. The theoretical prediction is confirmed by experimental observations as shown in Fig. 4 (see also Movie S2 in the Supplemental Material [24]), where glass spheres with diameters of 230–300 μm and tin spheres with diameters of 210–250 μm are mixed together on the specimen holder. When the acoustic power is 39 W, all the glass spheres can be stably trapped on the surface of the PCP, and only the tin particles stay on the specimen holder, as shown in Fig. 4(c).

In conclusion, we achieve tunable aligning, trapping, sieving, and transferring of many particles under a thin plate by using a PCP driven by a US plane wave. The acoustic trapping force originates from the sharp acoustic radiation force gradients based on the nonleaky A_0 Lamb mode of an immersed thin plate. The size of these manipulated particles is smaller than the spatial period of the stubs (p), and p is the wavelength of the corresponding A_0 mode which is less than the wavelength of US in water. Thus, subwavelength particles can be trapped by a PCP. Furthermore, since the resonance frequency of the patterned structure is geometrically dependent on the ratio of the plate thickness to the structural period [20], the exciting frequency of the trapping force can be controlled and the sizes of the particles to be sieved could be met by design. The net trapping force is dependent on the acoustic power, frequency of US, diameter, and mass density of the particles, and the PCP structure can be used for sieving subwavelength particles with different sizes or densities by tuning the driving acoustic power. Additionally, since the trapping surface is flat, the patterned structure can be easily integrated with a conventional microfabrication process such as microelectromechanical systems technology. This acoustic sieve demonstrates the effective manipulation of massive particles using an artificially engineered acoustic field, and we believe it has potential applications ranging from biomedical engineering to additive manufacturing.

This research was supported by the National Natural Science Foundation of China (NSFC Grants No. 81027006, No. 11274008, No. 10904094, No. 61020106008, No. 11325420) and 973 Research Program of China

(Grant No. 2010CB534914). F. C. was partially supported by Beijing Center for Mathematics and Information Interdisciplinary Sciences, and Shenzhen Key Lab for Molecular Imaging.

F. L. and F. C. contributed equally to this work.

[1] K. Ferrara, R. Pollard, and M. Borden, Ultrasound microbubble contrast agents: Fundamentals and application to gene and drug delivery, Annu. Rev. Biomed. Eng. **9**, 415 (2007).

[2] D. T. Pham and S. S. Dimov, *Rapid Manufacturing: The Technologies and Applications of Rapid Prototyping and Rapid Tooling* (Springer, London, 2000).

[3] A. Ashkin and J. M. Dziedzic, Optical trapping and manipulation of viruses and bacteria, Science **235**, 1517 (1987).

[4] M. P. MacDonald, L. Paterson, K. Volke-Sepulveda, J. Arlt, W. Sibbett, and K. Dholakia, Creation and manipulation of three-dimensional optically trapped structures, Science **296**, 1101 (2002).

[5] J. D. Thompson, T. G. Tiecke, N. P. de Leon, J. Feist, A. V. Akimov, M. Gullans, A. S. Zibrov, V. Vuletic, and M. D. Lukin, Coupling a single trapped atom to a nanoscale optical cavity, Science **340**, 1202 (2013).

[6] F. M. Fazal and S. M. Block, Optical tweezers study life under tension, Nat. Photonics **5**, 318 (2011).

[7] M. C. Zhong, X. B. Wei, J. H. Zhou, Z. Q. Wang, and Y. M. Li, Trapping red blood cells in living animals using optical tweezers, Nat. Commun. **4**, 1768 (2013).

[8] J. Wu, Acoustical tweezers, J. Acoust. Soc. Am. **89**, 2140 (1991).

[9] J. Shi, D. Ahmed, X. Mao, S. C. S. Lin, A. Lawit, and T. J. Huang, Acoustic tweezers: Patterning cells and microparticles using standing surface acoustic waves (SSAW), Lab Chip **9**, 2890 (2009).

[10] J. Lee, S. Y. Teh, A. Lee, H. H. Kim, C. Lee, and K. K. Shung, Single beam acoustic trapping, Appl. Phys. Lett. **95**, 073701 (2009).

[11] A. Lenshof, C. Magnusson, and T. Laurell, Acoustofluidics 8: Applications of acoustophoresis in continuous flow microsystems, Lab Chip **12**, 1210 (2012).

[12] J. P. Black, R. M. White, and J. W. Grate, Microsphere capture and perfusion in microchannels using flexural plate wave structures, in *Proceedings of the IEEE Ultrasonics Symposium, Munich, 2002*, edited by D. E. Yuhas and S. C. Schneider (IEEE, New York, 2002), p. 475.

[13] A. Haake, A. Neild, G. Radziwill, and J. Dual, Positioning, displacement, and localization of cells using ultrasonic forces, Biotechnol. Bioeng. **92**, 8 (2005).

[14] M. L. Juan, R. Gordon, Y. Pang, F. Eftekhari, and R. Quidant, Self-induced back-action optical trapping of dielectric nanoparticles, Nat. Phys. **5**, 915 (2009).

[15] J. H. Kang, K. Kim, H. S. Ee, Y. H. Lee, T. Y. Yoon, M. K. Seo, and H. G. Park, Low-power nano-optical vortex trapping via plasmonic diabolo nanoantennas, Nat. Commun. **2**, 582 (2011).

[16] S. Mandal, X. Serey, and D. Erickson, Nanomanipulation using silicon photonic crystal resonators, Nano Lett. **10**, 99 (2010).

[17] A. H. J. Yang, S. D. Moore, B. S. Schmidt, M. Klug, M. Lipson, and D. Erickson, Optical manipulation of nanoparticles and biomolecules in sub-wavelength slot waveguides, Nature (London) **457**, 71 (2009).

[18] Y. Pang and R. Gordon, Optical trapping of a single protein, Nano Lett. **12**, 402 (2012).

[19] X. Ding, S. C. S. Lin, B. Kiraly, H. Yue, S. Li, I. K. Chiang, J. Shi, S. J. Benkovic, and T. J. Huang, On-chip manipulation of single microparticles, cells, and organisms using surface acoustic waves, Proc. Natl. Acad. Sci. U.S.A. **109**, 11105 (2012).

[20] Z. He, H. Jia, C. Qiu, S. Peng, X. Mei, F. Cai, P. Peng, M. Ke, and Z. Liu, Acoustic transmission enhancement through a periodically structured stiff plate without any opening, Phys. Rev. Lett. **105**, 074301 (2010).

[21] F. Cai, Z. He, Z. Liu, L. Meng, X. Cheng, and H. Zheng, Acoustic trapping of particle by a periodically structured stiff plate, Appl. Phys. Lett. **99**, 253505 (2011).

[22] M. L. Juan, M. Righini, and R. Quidant, Plasmon nano-optical tweezers, Nat. Photonics **5**, 349 (2011).

[23] L. E. Kinsler, A. R. Frey, A. B. Coppens, and J. V. Sanders, *Fundamentals of Acoustics* (John Wiley and Sons, New York, 2000).

[24] See Supplemental Material at http://link.aps.org/supplemental/10.1103/PhysRevApplied.1.051001 for Supplemental Movie S1, Supplemental Movie S2, and supplemental information regarding experimental setup and numerical calculations.

[25] G. S. Settels, *Schlieren and Shadowgraph Techniques: Visualizing Phenomena in Transparent Media* (Springer, Heidelberg, 2001).

[26] T. A. Pitts and J. F. Greenleaf, Three-dimensional optical measurement of instantaneous pressure, J. Acoust. Soc. Am. **108**, 2873 (2000).

[27] F. Cai, L. Meng, C. Jiang, Y. Pan, and H. Zheng, Computation of the acoustic radiation force using the finite-difference time-domain method, J. Acoust. Soc. Am. **128**, 1617 (2010).

[28] T. Hasegawa and K. Yosioka, Acoustic-radiation force on a solid elastic sphere, J. Acoust. Soc. Am. **46**, 1139 (1969).